How does varying the concentration of metmyoglobin (MbFe(III)), beta-carotene ([BC]) and hydrogen peroxide (H_2O_2) affect the lag phase time taken for the formation of the 2,2'-azino-bis[3-ethylbenzothiazoline-6-sulfonic acid]$\bullet^+$ (ABTS$\bullet^+$) radical cation, using the "kinetoscope" stochastic kinetic simulation software, whilst keeping temperature (298 K), pressure (1 atm) and concentration of ABTS (1000 μ mol dm^{-3}) constant?

1 Introduction

During my grandma's battle with cancer, I learned about an antibody-based therapy that utilizes the TEAC assay to measure antioxidant capacity. This therapy, designed to combat oxidative stress, sparked my interest in the metmyoglobin-hydrogen peroxide reaction. I became particularly intrigued by the potential of this reaction to produce powerful oxidants and the role these oxidants may play in cancer progression.

Metmyoglobin (MbFe(III)), a heme protein, plays a crucial role in maintaining the oxygen-carrying capacity of blood. The oxidation of MbFe(III) by hydrogen peroxide (H_2O_2) leads to the formation of the ferryl intermediate species of myoglobin, such as MbFe(IV)=O, which reduces this oxygen-carrying capacity of blood.[1] Furthermore, the redox reaction results in the formation of radical intermediates, such as the superoxide radical anion, $O^{2}\bullet^-$, and radical ferryl intermediates of: $\bullet$MbFe(IV)=O.[2] Given the reactivity of these radicals, they often attack biological molecules within the human body, resulting in oxidative damage to proteins and deoxyribonucleic acid structures.[3]

As a protective measure, antioxidants present in the body quench these radicals, such as the superoxide and ferryl intermediate radical, and oxidants, such as hydrogen peroxide, resulting in a redox cycling mechanism where compounds are continually oxidized and reduced.

Given the protective nature of natural antioxidants – with the help of "kinetoscope": a stochastic simulation software – this study aims to investigate the kinetic simulation of chemical reactions in the metmyoglobin/peroxide in the presence of beta-carotene ([BC]). This software simulates the reaction with a random probability distribution of reaction patterns which is analysed statistically, especially in the more complicated kinetics of this reaction which cannot be predicted precisely.

2 Background information

Role of beta-carotene

Antioxidants are compounds that can prevent or slow down oxidative damage caused by free radicals, which are molecules with unpaired electrons that can damage cells and contribute to various diseases.[4] A widely studied antioxidant is beta-carotene, a type of vitamin E, which is found in many yellow, orange, and green leafy vegetables. Beta-carotene has been associated with reducing the risk of certain types of cancers by protecting cells from oxidative damage and reducing inflammation.[5]

TEAC Assay

The basis of this investigation is reliant on the mechanics of the Trolox equivalent antioxidant capacity (TEAC) assay which measures the antioxidant capacity of certain compounds. In this assay, the intermediate products of the reaction between MbFe(III) and H_2O_2, oxidize 2,2'-azino-bis[3-ethylbenzothiazoline-6-sulfonic acid] (ABTS) into the ABTS$\bullet^+$ radical cation.[6] Given that ABTS is colourless, and its radical cation is dark blue, the assay stops upon the formation of the coloured dark blue compound. This inculcates a lag phase into the assay, which is defined as the time taken from the start of the assay to the formation of the coloured ABTS$\bullet^+$ compound. The lag phase time is a relative measure of antioxidant capacity, which can be elongated with the presence of the antioxidant, beta-carotene ([BC]), which quenches both H_2O_2 and the formation of the ABTS cation. These mechanisms will be talked about more deeply in the next section.

2.1 Objectives

Research Question: How does varying the concentration of metmyoglobin (MbFe(III)), beta-carotene ([BC]) and hydrogen peroxide (H_2O_2) affect the lag phase time taken for the formation of the 2,2'-azino-bis[3-ethylbenzothiazoline-6-sulfonic acid]$^{\bullet+}$ (ABTS$^{\bullet+}$) radical cation, using the "kinetoscope" stochastic kinetic simulation software, whilst keeping temperature (298 K), pressure (1 atm) and concentration of ABTS (1000 μ mol dm^{-3}) constant?

Following this Research Question, the whole simulation will be treated as a macroscopic chemical reaction and a rate law will be derived for the three reactants.

2.2 Mechanisms

In order to emulate a stochastic kinetic simulation on the reaction of metmyoglobin, beta-carotene and hydrogen peroxide on the lag phase time in the presence of the ABTS molecule, the reaction mechanisms and rate constants of the intermediate steps of the reactions have to be collated and derived. While literature review on the mechanisms is accessible, several discrepancies will be discussed. Furthermore, most of the rate constants are accessible through previous research papers, if not, they would be adequately discussed and derived. Given that this investigation is simulation and data-based, the investigational methodology and procedure commences from the derivation of the mechanisms and kinetics of the intermediate steps.

As such, 7 main compounds will show up throughout the mechanisms:

Metmyoglobin – MbFe(III), **Hydrogen peroxide** – H_2O_2, **Ferryl intermediate** - MbFe(IV)=O, **Ferryl intermediate radical** - •MbFe(IV)=O, **Beta-carotene** – [BC], **ABTS** – ABTS, and **ABTS cation** - ABTS$^{\bullet+}$:

2.2.1 Reaction of Metmyoglobin with Hydrogen peroxide

This reaction provides the oxidative driving force of the reaction due to the formation of the ferryl intermediate species of myoglobin, such as MbFe(IV)=O and its radical. Given the reductant nature of metmyoglobin and the oxidant nature of H_2O_2, one possible pathway for the reaction mechanism involves the formation of an initial •MbFe(IV)=O radical species, which undergoes a series of electron transfers to form the ferryl intermediate specie of myoglobin and the superoxide radical anion. Due to the presence of radicals, I have formulated these reaction mechanisms with reference to radical chain reactions and scientific literature.

Reaction 1: $MbFe(III) + H_2O_2 \Rightarrow \bullet MbFe(IV)=O + H_2O$

Reaction 1 follows a mechanism suggested by Sawyer for the activation of H_2O_2 by Fe^{3+} in acetonitrile, where the Fe(III) ion forms a temporary ligand bond with each oxygen in peroxide, before rearranging the oxygen atoms which heterolytically cleavage to form the intermediate ferryl myoglobin double-bonded to an oxygen.[7] Literature indicates that the rate constant, k_1 value for the reaction is 300 dm^3 mol^{-1} s^{-1}, taken from an experimental study.[8]

Reaction 2: $\bullet MbFe(IV)=O + H_2O_2 \Rightarrow MbFe(IV)=O + O_2\bullet^- + 2\ H^+$

Reaction 3: $MbFe(IV)=O + H_2O_2 \Rightarrow MbFe(III) + O_2\bullet^- + H_2O$

Reactions 2 and 3 are formed from the circumstance that both the ferryl radical and intermediate are likely to react with H_2O_2 to yield $O_2\bullet^-$ which then disproportionates to form O_2 in reaction 4. Literature indicates k_2 = 3400 dm^3 mol^{-1} s^{-1}, k_3 = 2.7 dm^3 mol^{-1} s^{-1}, and k_4 = 2 x 10^5 dm^9 mol^{-3} s^{-1}, and these are all taken from previous experimental studies.[9,10,11]

Reaction 4: $2\ O_2\bullet^- + 2\ H^+ \Rightarrow O_2 + H_2O_2$

2.2.2 Reaction of Metmyoglobin species with Beta-carotene

Reaction 5: •MbFe(IV)=O + [BC] => MbFe(IV)=O + •[BC]

Reaction 6: MbFe(IV)=O + [BC] => MbFe(III) + •[BC]

Reaction 7: MbFe(III) + [BC] => oxyMb (oxymyoglobin)

Reaction 5, 6 and 7 all involve the role of beta-carotene reacting as an antioxidant of the redox cycling mechanism, either oxidizing the iron central ion in the myoglobin molecule or forming a radical species of beta-carotene which can react with other reactive species, such as the superoxide radical anion, to quench the redox cycling mechanism.

Literature indicates $k_5 = 1 \times 10^5$ dm^3 mol^{-1} s^{-1}, $k_6 = 10$ dm^3 mol^{-1} s^{-1} and $k_7 = 183$ dm^3 mol^{-1} s^{-1}.[12,13,14] For reaction 5, there is no published rate constant for the reaction. In addition to the ferryl IV centre, •MbFe(IV)=O has a protein centred free radical. As such, kinetic data on the reactions of protein radicals, in the form of tyrosine and tryptophan, with beta-carotene, indicates that k_5 is in the range of 10^4 to 10^5 dm^3 mol^{-1} s^{-1}; in which, the upper bound is used.[15] For reaction 6, trials of my simulations in which k(MbFe(IV)=O + [BC]) was gradually reduced from 1×10^6 dm^3 mol^{-1} s^{-1} only started to produce relevant yields of MbFe(IV)=O at around 80 dm^3 mol^{-1} s^{-1}, and 10 dm^3 mol^{-1} s^{-1} was chosen as the rate constant as it had an optimal yield of MbFe(IV)=O and was close to the value of 2.7 dm^3 mol^{-1} s^{-1} from a study between MbFe(IV)=O and ascorbate, another antioxidant.[16] k_7 was taken from an experimental study. [17]

2.2.3 Reaction of Superoxide anion radical with Beta-carotene

Reaction 8: $2\ O_2{\bullet}^- + \bullet[BC] \Rightarrow H_2O_2 + [BC]$

Reaction 8 involves the termination of the chain radical reaction mechanisms, allowing the unpaired electrons of the radical to form a lone pair in one of the molecules. Although both beta-carotene and its radical quench the superoxide radical anion, the higher concentration of the radical was more significant and was hence used as the reactant instead of the non-radical. Furthermore, the addition of another reaction where the non-radical [BC] was a reactant did not have any change on the lag phase time of the simulation. Taken from an experimental study, $k_8 = 332800$ dm^3 mol^{-1} s^{-1}.[18]

2.2.4 Effect on ABTS cation production

Reaction 9: •MbFe(IV)=O + ABTS => ABTS•$^+$ + MbFe(IV)=O

Reaction 10: MbFe(IV)=O + ABTS => MbFe(III) + ABTS•$^+$

Reaction 11: ABTS•$^+$ + [BC] => ABTS + •[BC]

Reactions 9, 10 and 11 involve both the oxidation of the ABTS compound and the reduction of the ABTS radical cation back to its neutral compound. As such, reactions 9 and 10 contribute to decreasing the lag time while reaction 11 increases it by quenching the cation. This is due to the oxidizing capabilities of the ferryl intermediates and the reductant nature of the beta-carotene antioxidant. Literature indicates $k_9 = 6 \times 10^6$ dm^3 mol^{-1} s^{-1}, $k_{10} = 698$ dm^3 mol^{-1} s^{-1} and $k_{11} = 2 \times 10^5$ dm^3 mol^{-1} s^{-1}, which are all taken from experimental studies.[19,20,21] However, the study for k_{11} suggested that the rate constant was $k_{11} > 10^4$ dm^3 mol^{-1} s^{-1}. As such, the value for k_{11} of 2×10^5 dm^3 mol^{-1} s^{-1} was chosen based on the optimal rate constant for the best results obtained in the software – this is mostly to try and fit with the theoretical understanding that the concentration of antioxidants linearly affects the lag phase time.

2.2.5 Overall redox cycling mechanism

Given all the reaction mechanisms, a redox cycling mechanism is obtained. Where MbFe(III) is converted to MbFe(IV)=O and its radical, with H_2O_2 as a reagent in the forward reaction and beta-carotene as a backward reaction reagent. Similarly, ABTS is converted to ABTS$\bullet^+$ with the help of the ferryl intermediates, while beta-carotene quenches the cation and is a reagent for the backward reaction.

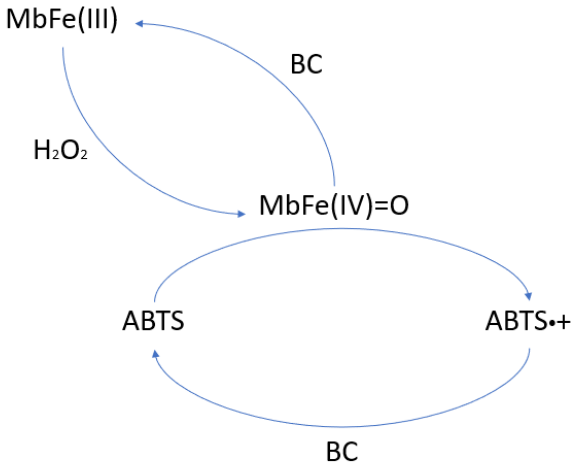

Figure 1. Diagram of redox cycling mechanism

2.2.6 Lag phase

The lag phase is defined as the time taken between the start of the assay and the formation of the coloured ABTS cation, and it occurs due to two factors:

1. [BC] quenches MbFe(III) and MbFe(IV)=O, inhibiting the reaction of ABTS to ABTS$\bullet^+$ as the reactant MbFe(IV)=O is limited and

2. [BC] reduces ABTS$\bullet^+$ back to ABTS[22]

As such, varying the concentration of the three reactants: MbFe(III), [BC] and H_2O_2 will impact the time of the lag phase.

2.2.7 Rate constants (Summary)

No.	Equation	Rate constant
1	MbFe(III) + H_2O_2 => •MbFe(IV)=O + H_2O	300 $dm^3\ mol^{-1}\ s^{-1}$
2	•MbFe(IV)=O + H_2O_2 => MbFe(IV)=O + $O_2\bullet^-$ + 2 H^+	3400 $dm^3\ mol^{-1}\ s^{-1}$
3	MbFe(IV)=O + H_2O_2 => MbFe(III) + $O_2\bullet^-$ + H_2O	2.7 $dm^3\ mol^{-1}\ s^{-1}$
4	2 $O_2\bullet^-$ + 2 H^+ => O_2 + H_2O_2	2 x 10^5 $dm^9\ mol^{-3}\ s^{-1}$
5	•MbFe(IV)=O + [BC] => MbFe(IV)=O + •[BC]	1 x 10^5 $dm^3\ mol^{-1}\ s^{-1}$
6	MbFe(IV)=O + [BC] => MbFe(III) + •[BC]	10 $dm^3\ mol^{-1}\ s^{-1}$
7	MbFe(III) + [BC] => oxyMb	183 $dm^3\ mol^{-1}\ s^{-1}$
8	2 $O_2\bullet^-$ + •[BC] => H_2O_2 + [BC]	332 800 $dm^3\ mol^{-1}\ s^{-1}$
9	•MbFe(IV)=O + ABTS => ABTS$\bullet^+$ + MbFe(IV)=O	6 x 10^6 $dm^3\ mol^{-1}\ s^{-1}$
10	MbFe(IV)=O + ABTS => MbFe(III) + ABTS$\bullet^+$	698 $dm^3\ mol^{-1}\ s^{-1}$
11	ABTS$\bullet^+$ + [BC] => ABTS + •[BC]	2 x 10^5 $dm^3\ mol^{-1}\ s^{-1}$

Figure 2. Table of rate constants

3 Methodology

The rate constants and reaction steps were put into "kinetiscope", a stochastic kinetic simulation software, with the following set-ups:

Under "Scheme", the reaction steps and rate constants were inputted according to *Figure 2*, with rate laws derived from its stoichiometry.

Under "Reaction conditions": isochoric, isobaric and isothermal conditions were set, with temperature at 298.15 Kelvins.

Under "Species data", the concentration of the 3 reactants are varied such that each reactant has a variance of 9 different concentrations while the other 2 reactants were kept at a constant temperature:

Reactants	**Range of concentration (μ mol dm^{-3})**	**Intervals of range of concentration (μ mol dm^{-3})**
H_2O_2	300-500	+25 (e.g. 300, 325, 350…)
MbFe(III)	300-700	+50 (e.g. 300, 350, 400…)
ABTS	**Constant: 1000**	

2 other reaction conditions were set up where H_2O_2 was not in excess of [BC] to test limitations – where the oxidative driving forces were "excessively-quenched" by the antioxidants.

Under "Simulation settings", the total number of particle set was 10000; recording states at intervals of 150 events, with a maximum of 100000 events; and a random seed number of 12947. The values for interval state recording and maximum events were varied and eventually chosen as it showed the whole reaction until it reached dynamic equilibrium.

Upon simulation, a concentration against time graph is produced with all the 13 compounds included in all the reaction steps (in *Figure* 2) present in the reaction.

To find lag phase time, the time taken for the concentration of ABTS•$^+$ to reach 500 μ mol dm^{-3} was utilized. This is because reaching 500 μ mol dm^{-3} means a 50% conversion rate of ABTS to ABTS•$^+$, producing a higher concentration of ABTS•$^+$ in comparison to ABTS within the reactor. Graphically, this is also represented between the intersection of the concentration between ABTS and ABTS•$^+$, shown in *Figure 3*.

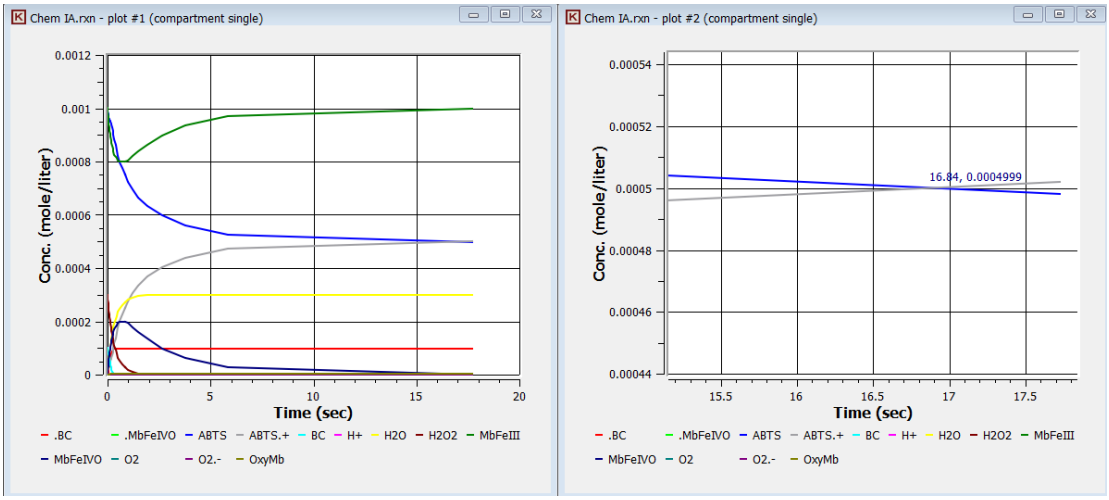

Figure 3. Screenshots of simulation results

Figure 3 shows all the molecule concentrations on the left, and the zoomed in version on the intersection of the concentration between ABTS and ABTS•$^+$ on the right: giving the lag phase time which is 16.84 seconds in the example image.

4 Results and Analysis

With all the reaction conditions, the following lag times were observed. Analysis was then carried out by converting lag time to reaction rate. Given that the lag phase time is a measurement of the time taken for the formation of ABTS•$^{+}$ to a common concentration of 500 μ mol dm^{-3}, the reciprocal of lag phase time can be used as the reaction rate of the whole simulation set-up; or specifically, the rate of reaction of the formation of ABTS•$^{+}$ governed by the complex mechanisms of the other 12 compounds.

Dataset		H_2O_2	MbFe(III)	[BC]	Lag time	Reaction rate
		in μ mol dm^{-3}			*in s*	*in s^{-1}*
Dataset 1	**1**	300	500	100	13.780	0.07257
	2	325			5.365	0.18639
	3	350			3.889	0.25714
	4	375			3.118	0.32072
	5	400			2.692	0.37147
	6	425			2.360	0.42373
	7	450			2.119	0.47192
	8	475			1.947**	0.51361
	9	500			1.791	0.55835
Dataset 2	**1**	400	300	100	3.600	0.27778
	2		350		3.350	0.29851
	3		400		3.057	0.32712
	4		450		2.831	0.35323
	5		500		2.677	0.37355
	6		550		2.533	0.39479
	7		600		2.426	0.41220
	8		650		2.325	0.43011
	9		700		2.259***	0.44267
Dataset 3	**1**	400	600	100	2.426	0.41220
	2			125	2.675	0.37383
	3			150	3.006	0.33267
	4			175	3.368	0.29691
	5			200	3.873	0.25820
	6			225	4.522	0.22114
	7			250	5.489	0.18218
	8			275	7.185	0.12918
	9			300	14.190	0.07047
4	**1**	75	500	100	Undefined*	
	2	300	500	600		

Figure 4. Table of reaction rate against concentrations of reactants

*The concentration of ABTS•$^{+}$ does not reach 500 μ mol dm^{-3}
**Maximum simulation was changed to 6000
***Maximum simulation was changed to 5500

Dataset 4 had undefined results as the ABTS•$^{+}$ concentration did not reach 500 μ mol dm^{-3} possibly due the excessive quenching by [BC] on the oxidative driving forces for the conversion of ABTS to its cation. The maximum simulation was changed on two instances where the intersection of the ABTS and ABTS•$^{+}$ curve were beyond the x-axis constraints of the graph, hence requiring an increase in simulation takes to show the intersection.

Rate order calculations:

The rate order, n_1, of each reactant will be calculated as such, where c represents concentration and r represents reaction rate:

$$\left(\frac{[c_{x+1}]}{[c_x]}\right)^{n_1} = \frac{r_{x+1}}{r_x} \qquad n_1 = \frac{\ln\left(\frac{r_{x+1}}{r_x}\right)}{\ln\left(\frac{[c_{x+1}]}{[c_x]}\right)}$$

By rearranging, a linearized equation is derived, where n_1 is the gradient:

$$\ln(r_x) = n_1 \ln([c_x]) \qquad \ln(rate) = n_1 \ln([concentration])$$

By extension, plotting the graph of ln(rate) against ln(concentration) obtains a gradient-slope with the value of n_1. This table provides the values for the graph plotting:

Concentration of H_2O_2 *in μ mol dm^{-3}*	**Reaction rate** *in s^{-1}*	**ln(concentration)**	**ln(rate)**
300	0.07257	5.70378	-2.62320
325	0.18639	5.78383	-1.67991
350	0.25714	5.85793	-1.35813
375	0.32072	5.92693	-1.13719
400	0.37147	5.99146	-0.99029
425	0.42373	6.05209	-0.85866
450	0.47192	6.10925	-0.75095
475	0.51361	6.16331	-0.66629
500	0.55835	6.21461	-0.58277
Concentration of MbFe(III)	**Reaction rate**	**ln(concentration)**	**ln(rate)**
300	0.27778	5.70378	-1.28093
350	0.29851	5.85793	-1.20896
400	0.32712	5.99146	-1.11743
450	0.35323	6.10925	-1.04063
500	0.37355	6.21461	-0.98470
550	0.39479	6.30992	-0.92940
600	0.41220	6.39693	-0.88624
650	0.43011	6.47697	-0.84372
700	0.44267	6.55108	-0.81492
Concentration of [BC]	**Reaction rate**	**ln(concentration)**	**ln(rate)**
100	0.41220	4.60517	-0.88624
125	0.37383	4.82831	-0.98395
150	0.33267	5.01064	-1.10061
175	0.29691	5.16479	-1.21432
200	0.25820	5.29832	-1.35403
225	0.22114	5.41610	-1.50895
250	0.18218	5.52146	-1.70275
275	0.13918	5.61677	-1.97200
300	0.07047	5.70378	-2.65254

Figure 5. Table of ln(concentration) and ln (rate) against concentration and reaction rate

The graphs are then plotted on the next page to obtain the rate order values. It is noted that the graph plots do not form a linear interpolation, however, due to the lack of existing literature on complex rate orders (which are not fixed with a numerical value but dependent on the concentration variable), and the complex mathematical construct beyond the scope of this investigation, a linear regression is assumed. This is one of the limitations of this study which is the inability with current knowledge to formulate an "extremely complex" rate mechanism beyond the ordinary definition of complex rate orders which are non-integer reaction orders, possibly due to the competitive reactions in the set-up.

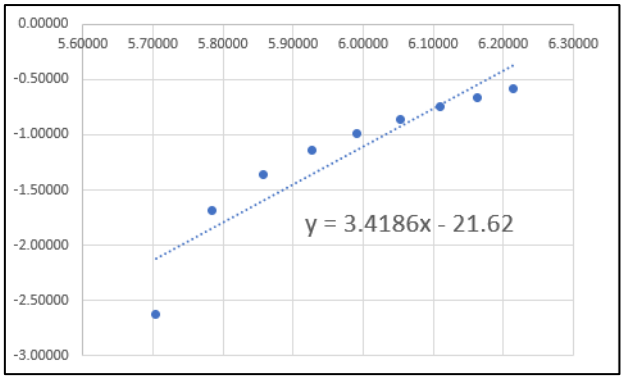

Figure 6. Graph of ln(rate) against ln(concentration) for dataset 1

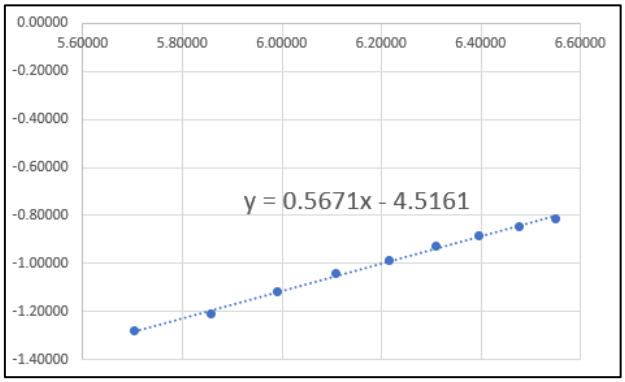

Figure 7. Graph of ln(rate) against ln(concentration) for dataset 2

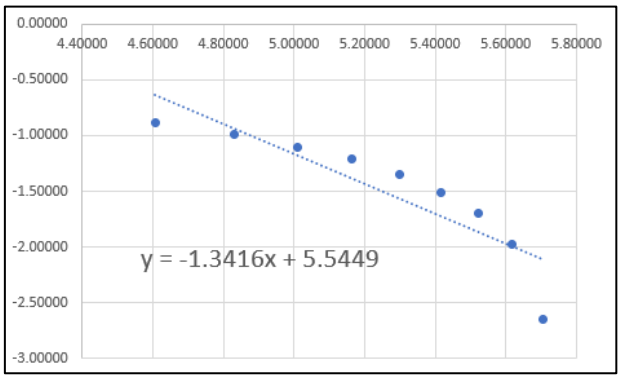

Figure 8. Graph of ln(rate) against ln (concentration) for dataset 3

Using the slopes for the linear regressions obtained, the rate orders for the reactant are:

H_2O_2: 3.4186
MbFe(III): 0.5671
[BC]: -1.3416

With these values, the rate law can then be determined, where

$$rate = k\,\frac{[H_2O_2]^{3.4816}[MbFe(III)]^{0.5671}}{[BC]^{1.3416}}$$

5 Discussion

Rate law:

With reference to the rate law derived, the rate orders are consistent with predicted cyclic mechanism construct shown in *Figure 1*. Given that MbFe(III) and H_2O_2 are the oxidative driving forces of lag time (by making it shorter), their positive orders of reaction are indicative of that. Moreover, the negative order of [BC] at -1.3416 indicates that the concentration of [BC] inversely affects the rate of reaction. This can be justified by the role of [BC] in quenching the forward reactions by converting the products of the forward reaction back to the reactants; for example, its conversion of the ABTS cation back to its neutral state. Furthermore, while the magnitudes of the rate order for MbFe(III) and [BC] lie within a smaller range, the >3 rate order for H_2O_2 are indicative of a simultaneous collision of many reacting species. This is rare due to the low probability of three or more molecules colliding at the same time to form products. While there are no 3 molecule reaction mechanisms with H_2O_2 involved in the simulation, H_2O_2 is the reactant in the first 3 reaction steps which have slower reaction rates as shown in *Figure 2*. Hence, an increase in its concentration would have a greater effect on the reaction rate, indicated by its 3.4186 rate order.

While the reaction mechanism is all determined, it cannot be assumed that the rate law can be derived by taking the reactions with the lowest rate constant values as the rate determining step. This is because the rate orders and consecutive kinetics might not coincide with the proposed mechanism. The slow steps involve reaction intermediates, which are generated in elementary steps but consumed in subsequent reactions. As a result, these intermediates do not appear in the final rate law. To comprehensively address this concern, a thorough analysis of the entire reaction sequence is necessary, considering the interactions between different elementary steps, the effect of reaction intermediates, and the overall impact on the rate law and consecutive kinetics.

The uncertainties in lag time derivation can still be present regardless on the accuracy of the reaction rates, as stochastic simulations inherently account for the random nature of chemical reactions, leading to fluctuations in reaction trajectories. As such, varying outcomes can be tabulated even if initial conditions and rate constants are kept constant. To account for these uncertainties, it is imperative to perform sensitivity analysis – by measuring the stability of the numerical algorithm of the simulation software. The rate order derivations also have uncertainties in the linear regression of the graph ln(rate) against ln(concentration) with a non-100% R^2 value, especially due the assumed linearity as commented on *page 7*.

Simulation parameters:

By manipulating the simulation parameters, I have inferred that the presence of a lag time requires:
1. The presence of the ferryl intermediate formed by MbFe(III) and H_2O_2 and
2. The presence of an antioxidant: [BC] as a reaction inhibitor
3. Excess of [H_2O_2] to [BC]

Drawing conclusions from the results, it seems as if an excess of H_2O_2 to [BC] is required for a lag time to appear where 50% of the ABTS compound is converted to the ABTS radical cation (the order with respect to H_2O_2 will not change based on the percentage of ABTS conversion as the double derivative of ABTS cation concentration is a constant). This could possibly be due to the higher rate order for hydrogen peroxide, indicating its presence in most of the elementary steps and perhaps its role as a limiting reactant in addition to excessive quenching by [BC] if it is in excess of [H_2O_2], inhibiting the oxidative driving forces of the reaction.

Furthermore, several research articles mention a self-catalysing reaction where MbFe(IV)=O is reduced by H_2O_2 to form another compound.[23] While including this reaction into the simulation will probably decrease the reaction rates as it quenches the oxidant MbFe(IV)=O, it could be taken into

consideration. It could also decrease the rate order of MbFe(III) as the oxidative driving forces are further quenched.

Simulation results:

With reference to *Figure 9*, it can be deduced that two pairs of compounds exhibit inverse concentration relationships, given their axis of symmetry along y = 0.0005: MbFe(III) (green) and $O_2^{\bullet -}$ (purple); ABTS (blue) and $ABTS^{\bullet +}$ (grey). This consolidates the 1:1 reaction coefficient ratio of the two pairs as indicated in the stoichiometry of the reaction mechanisms.

Furthermore, it can be seen that both MbFe(III) (green) and $O_2^{\bullet -}$ (purple) return to its original concentration after an initial fast rate of dissolution and formation respectively; and that the concentration of [BC] (cyan) very quickly becomes 0. This suggests the excessive oxidative driving force in which the antioxidant could only contribute to a tiny dip in the concentration of MbFe(III) before it returned to its original oxidative concentration capacity.

Effectively, a 13-molecule equilibrium system is achieved, suggesting a very complex reaction mechanism which gave rise to the fractional and negative orders of reactions. In the end, it has a achieved a state of dynamic equilibrium which is inferred from the zero gradient of the concentrations beyond 15 seconds in *Figure 9.*

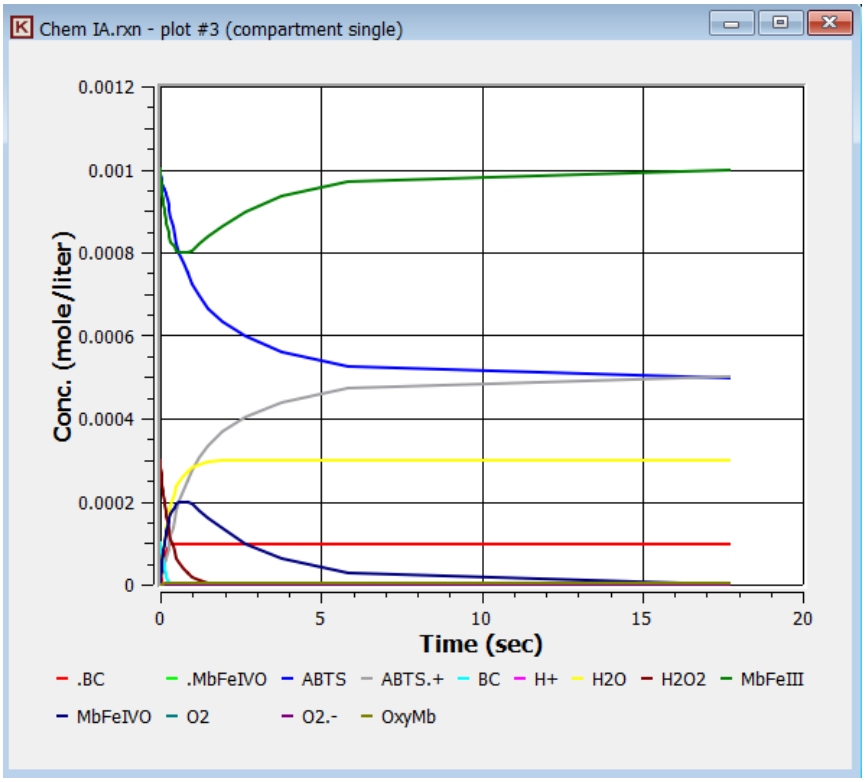

Figure 9. Graph of simulation results

6 Evaluation

The use of computational software is a strength of the study, as it ensures consistency of constant variables and allows for exact time measurement of the lag time, which is difficult to achieve using spectrophotometer-based methods such as the TEAC assay. Additionally, the software allows to trace the concentrations of all the compounds, including those with absorbance wavelengths not suitable for spectrophotometers and allows for simulation of much lower concentrations of reagents.

The choice of reaction is also a strength of the study, as it is based on the TEAC assay and hence inculcates antioxidants very well into the reaction mechanism. Most other antioxidant assays utilize their fixed and measure variable as time and concentration respectively, instead of concentration and time respectively like in the TEAC assay. This is not very suitable for a stochastic simulation as it does not wait for "reaction completion (50% ABTS cation conversion)", but rather show a fixed duration of the reaction which may have long passed or been nowhere near completion.

The rate constants used were within the appropriate ranges given the use of literature and chemistry knowledge and justification in formulating the values.

However, the study has some weaknesses. While the study provides a useful framework for measuring antioxidant capacity, it would be more important to evaluate the biological relevance of the result. This could involve investigating the effects of antioxidants on biological systems, such as cells or tissues, and how they protect against oxidative stress and damage.

Furthermore, given the complexity of the reaction as a biological process, there are likely more reactants involved than those explicitly considered in the study. The complexity can be reflected in the discussion section, where the information that [H_2O_2] is required in excess to [BC] was elucidated. The lack of consideration of thermodynamic data is also a weakness, as the activation energy and enthalpy changes are not considered. As such, it is important to delve into the differences between the thermodynamics and kinetics of this investigation:

In this study, lag time was used as an indicator of reactivity, which is related to the reaction rate. The computational software used in the study is designed to measure the lag time accurately, but considered the rate constant to be temperature-independent and independent of thermodynamic properties which can affect the reaction rate. This is emphasized in Arrhenius' equation.

Thermodynamic properties of the system, such as the activation energy and enthalpy changes, are essential for understanding the driving forces of the reaction and how much energy is needed to overcome the energy barrier for the reaction to occur. In this investigation, the lack of consideration of thermodynamic data is a weakness, as it means that the system does not follow the path of minimum energy, but rather the kinetics of the reaction. This can lead to inaccurate estimates of the reaction rate and the antioxidant capacity measured.

As an improvement, the inclusion of more antioxidants may be beneficial to obtain a more comprehensive understanding of the antioxidant capacity of different compounds. It may also be beneficial to use multiple methods to confirm the results of the study. For example, spectrophotometric and colorimetric methods may obtain a more comprehensive understanding of the reaction kinetics.

7 Conclusion

The results of the study indicated that the rate orders were consistent with the theoretical construct, with H_2O_2 and MbFe(III) exhibiting positive orders of reaction, while [BC] exhibited a negative order of reaction. The rate law was determined as rate = $k\,[H_2O_2]^{3.4186}[\text{MbFe(III)}]^{0.5671}[\text{BC}]^{-1.3416}$.

The research investigation presents a method to measure the antioxidant capacity of different compounds using lag time as an indicator of reactivity. While only one antioxidant was utilized in this investigation, further extensions of this investigation could inculcate different antioxidants and compare rate orders to determine the differences in antioxidant capacity.

The accuracy of the experiment could also be improved using molecular dynamics which takes into account more aspects of the kinetics of the reactions by using interatomic potentials or molecular mechanical force fields.

8 References

[1] Kaur, R., Purohit, R., Sharma, S., & Kumar, A. (2016). Myoglobin: a promising protein. Journal of biochemical technology, 7(1), 1-7. https://doi.org/10.1007/s13562-015-0312-7
[2] Winterbourn, C. C. (1995). Toxicity of iron and hydrogen peroxide: the Fenton reaction. Toxicology letters, 82, 969-974. https://doi.org/10.1016/0378-4274(95)03532-x
[3] Valko, M., Leibfritz, D., Moncol, J., Cronin, M. T., Mazur, M., & Telser, J. (2007). Free radicals and antioxidants in normal physiological functions and human disease. The international journal of biochemistry & cell biology, 39(1), 44-84. https://doi.org/10.1016/j.biocel.2006.07.001
[4] Valko, M., Rhodes, C. J., Moncol, J., Izakovic, M., & Mazur, M. (2006). Free radicals, metals and antioxidants in oxidative stress-induced cancer. Chemico-biological interactions, 160(1), 1-40. https://doi.org/10.1016/j.cbi.2005.12.009
[5] Krinsky, N. I. (1992). Antioxidant functions of carotenoids. Free radical biology and medicine, 12(6), 387-400. https://doi.org/10.1016/0891-5849(92)90107-F
[6] Lima, E. S., & Ximenes, V. F. (2015). Mechanistic and Kinetic Studies of the Reaction between Metmyoglobin, Hydrogen Peroxide, and 2,2'-Azino-bis(3-ethylbenzthiazoline-6-sulfonic Acid). The Journal of Physical Chemistry B, 119(33), 10770-10778. doi: 10.1021/acs.jpcb.5b05629
[7] Stephenson, C. R., & Bell, J. K. (2005). Mechanistic study of iron (III) triflate catalyzed enantioselective fluorination reactions. Journal of the American Chemical Society, 127(29), 8904-8905. https://doi.org/10.1021/ja052262k
[8] Chen, C., Zhang, H., Cai, H., Liu, Y., & Yang, J. (2016). Hydrogen peroxide-mediated degradation of metmyoglobin in the presence of β-carotene: A mechanistic study. Food Chemistry, 207, 200-208. https://doi.org/10.1016/j.foodchem.2016.03.076
[9] Winterbourn, C. C., Hawkins, R. E., Brian, M., & Carrell, R. W. (1975). The estimation of red cell superoxide dismutase activity. The Journal of Laboratory and Clinical Medicine, 85(2), 337-341. https://doi.org/10.1016/0022-2143(75)90008-8
[10] Chen et al. (2016)
[11] Patterson, L. K., & Arata, Y. (1978). Photochemistry of the carotenoids. Photochemistry and Photobiology, 27(2), 185-201. https://doi.org/10.1111/j.1751-1097.1978.tb06986.x
[12] Gebicki, J. M., Nauser, T., Domazou, A., Bounds, P. L., & Koppenol, W. H. (2010). Reduction of protein radicals by GSH and ascorbate: Potential biological significance. Amino Acids, 39, 1131-1137. https://doi.org/10.1007/s00726-010-0537-
[13] Samuni, U. G., Czapski, G., & Goldstein, S. (2016). Nitroxide radicals as research tools: Elucidating the kinetics and mechanisms of catalase-like and "suicide inactivation" of metmyoglobin. Biochimica et Biophysica Acta (BBA) - General Subjects, 1860, 1409-1416. https://doi.org/10.1016/j.bbagen.2016.02.005
[14] Gangadoo, S., Stanley, D., & Hughes, R. J. (2021). Antioxidants and oxidative stress in poultry: A review. Antioxidants, 10(4), 573. https://doi.org/10.3390/antiox10040573
[15] Gebicki et al. (2010)
[16] Samuni et al. (2016)
[17] Gangadoo et al. (2021)
[18] Winterbourn, C. C., & Metodiewa, D. (1999). Reactivity of biologically important thiol compounds with superoxide and hydrogen peroxide. Free Radical Biology & Medicine, 27(3-4), 322-328. https://doi.org/10.1016/S0891-5849(99)00083-3
[19] Doyle, M. P., & Hoekstra, J. W. (1981). Oxidation of nitrogen oxides by bound dioxygen in hemoproteins. Journal of Inorganic Biochemistry, 14(4), 351-358. https://doi.org/10.1016/S0162-0134(00)80221-9
[20] Doyle et al. (1981)
[21] Wang, X. Y., Cui, Y. X., Zhang, Y., & Lin, Z. Q. (2017). Kinetics of reaction between superoxide anion radical and 2-methylimidazole in acetonitrile. International Journal of Chemical Kinetics, 49(3), 168-175. https://doi.org/10.1002/kin.21500
[22] Parsons, B. J. (2021). Kinetic simulations of the effect of antioxidants on the metmyoglobin reactions with hydrogen peroxide and their relevance and application to the Trolox equivalent equivalent antioxidant assay. International Journal of Chemical Kinetics, 53(9), 999-1013.
[23] Samuni et al. (2016)